

# Thin AlN Film Resonators utilizing the Lowest order Symmetric Lamb mode: Further Developments

V. Yantchev\* and I. Katardjiev

Dept. Solid State Electronics, Uppsala University, Uppsala, Sweden  
[veya@angstrom.uu.se](mailto:veya@angstrom.uu.se) , URL: <http://hermes.teknikum.uu.se/~veya/>

**Abstract**— Thin film plate acoustic wave resonators utilizing the lowest order symmetric Lamb wave ( $S_0$ ) propagating in highly textured  $2\mu\text{m}$  thick Aluminum Nitride (AlN) membranes were successfully demonstrated for the first time [1]. Further the utilization of fast lateral modes in thin films has recently being targeted independently by other groups as well [2,3]. The unperturbed  $S_0$  mode in thin film AlN has an acoustic wave velocity in excess of 10 000 m/s with a weak dispersion and sufficient coupling. Q factors of around 1800 were demonstrated for 890 MHz one-port synchronous resonators operating in the vicinity of the upper stopband edge [1]. In this work an experimental study on the resonators' performance vs variety of design parameters is performed. Devices operating in the vicinity of the stopband center offering a Q of up to 3000 at a frequency of around 875 MHz are demonstrated. Further, micromachined 2-port longitudinally coupled thin film resonators utilizing the  $S_0$  mode are demonstrated for the first time.

## I. INTRODUCTION

The full utilization of the electro-acoustic concepts employing the thin film technology requires the implementation of laterally propagating modes which offer a number of unique features [4]. The development of integrated acoustic resonators operating in the lower frequency (0.5 MHz – 5 GHz) band as well as the development of other types of thin film based IC compatible electroacoustic devices (for instance delay lines, longitudinally coupled filters, sensors, two-port resonators etc.) is a challenging problem of great importance and potential. The latter inspired a number of studies on high velocity surface acoustic waves (HVSAW). The central frequency of a SAW based device is determined by the equation  $f = V/\lambda$ , where  $f$  is the central frequency,  $V$  is the phase velocity of the acoustic wave and  $\lambda$  is the acoustic wavelength, which in turn is defined by the electrode pitch in the interdigital transducer (IDT). Hence, high-resolution lithography and/or the use of high acoustic velocity materials are the two main approaches for the fabrication of high-frequency SAW devices. The thin film technology provides the opportunity to combine a piezoelectric film with a high-velocity non-piezoelectric

substrate thus defining a good platform for high frequency SAW devices. Initially HVSAWs propagating in AlN/Sapphire have been studied because of the excellent acoustic quality of the sapphire ( $\text{Al}_2\text{O}_3$ ). SAWs propagating in (0002)AlN/(0001) $\text{Al}_2\text{O}_3$  exhibit velocities as high as 5700 m/s and electromechanical couplings of around 0.2% [5]. The latter figures along with the possibility for achieving zero temperature coefficient of frequency made the AlN/ $\text{Al}_2\text{O}_3$  structure attractive. Recently a 5GHz SAW filter on AlN/ $\text{Al}_2\text{O}_3$  with good temperature stability has been demonstrated [6]. Another attractive HVSAW system is the AlN/Diamond since the Diamond provides the highest acoustic wave velocity in nature. The development of methods for the synthesis of polycrystalline diamond films brought the possibility of using AlN/Diamond/Si multilayer structures providing SAW velocities in excess of 10 000 m/s and electromechanical coupling of up to 1.2% [7-9]. Resonators and filters in the lower GHz range based on HVSAWs propagating on AlN/Diamond/Si have successfully been demonstrated [10, 11]. One major disadvantage of the HVSAW concept is its relatively high cost, the relatively strong dispersion and the increased losses emanating from the defects induced at the interfaces. Thus, the HVSAW loss factor in the AlN/Diamond/Si is in the range 0.03 to 0.05 dB/ $\lambda$  thus limiting the device Q to 600 at a frequency of 1GHz [11]. Another quite promising alternative to the HVSAWs has recently been successfully demonstrated [12-14]. It is based on the utilization of laterally propagating fast wave-guided modes in thin AlN membranes also known as plate waves. Thus, the plate waves observed as spurious and degrading in the thin film bulk acoustic resonators (FBAR) can be utilized for practical microwave applications.

In Fig. 1 the calculated dependence of the acoustic velocity on the AlN film thickness for the first two SAW modes in an AlN/Diamond layered structure as well as the 0<sup>th</sup> order symmetric lamb mode ( $S_0$ ) in a thin AlN membrane are shown. Clearly the  $S_0$  mode exhibits a low dispersion for membrane thicknesses below  $0.4\lambda$  and offering at the same time an acoustic wave velocity close to 10 000 m/s. Further

---

This work is supported by SSF and Vinnova through the ICTEA and the WISENET programmes, respectively

the  $S_0$  mode offers higher electromechanical couplings in comparison to the HVSAW as seen from Fig. 2a,b.

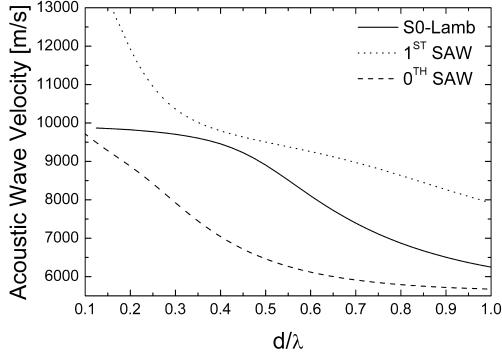
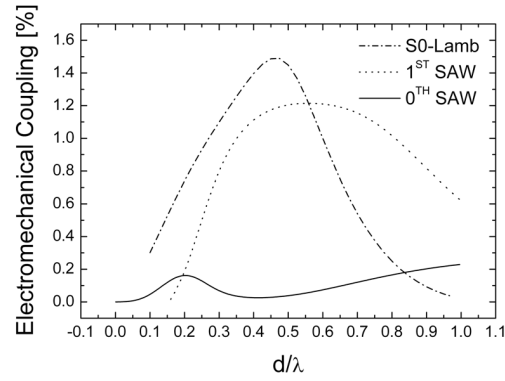
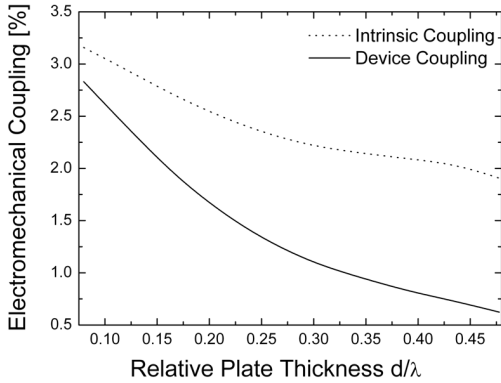


Figure 1. Velocities of the  $S_0$  Lamb wave and SAW modes as a function of  $d/\lambda$ , plate thickness to wavelength ratio, for c-oriented AlN thin film plates and AlN/Diamond layered structures respectively.



(a)



(b)

Figure 2. Calculated electromechanical couplings of the fast lateral modes as a function of the relative AlN thickness. a) Adler's approach [15], considering IDT type of excitation; b) Green function approach [16], considering longitudinal wave transducer utilizing lateral field excitation;

These unique properties of the Lamb waves make them attractive for the fabrication of IC compatible microwave components in the lower gigahertz range. Initial work on the

design and fabrication of high frequency resonators exploiting the  $S_0$  mode in thin AlN membranes has been reported recently [12, 13]. The results demonstrate the great potential of this mode and laid out the groundwork for further research in the field. On the other hand, as the authors point out, the device design employed was most likely not optimal due to insufficient knowledge of the propagation characteristics of the  $S_0$  mode under periodic strip gratings, which define the topology of the resonator. The theoretical analysis of the  $S_0$  propagation characteristics performed subsequently [17] indicates that it is possible to significantly optimize the Lamb wave resonant structures as subsequently demonstrated [1]. Q factors of around 1800 were demonstrated for 890 MHz one-port synchronous resonators operating in the vicinity of the upper stopband edge [1]. In here complementary efforts towards the design of thin film one-port Lamb wave resonators are presented. The effect of the device aperture on the device response is investigated and high Q designs of one-port thin film resonators are presented. Further Lamb wave two-port thin film resonators are designed and micromachined for the first time. Most generally the thin film Lamb wave technology is similar to the FBAR technology. The devices have been fabricated on a micro-machined freestanding AlN membrane. As a supporting substrate a (100) oriented low resistive (10  $\Omega\cdot\text{cm}$ ) 4-inch Si wafer has been used. After cleaning the substrate, a 2.2  $\mu\text{m}$  thick AlN film is deposited by reactive sputtering onto the bottom electrodes using a Von Ardenne reactive balanced magnetron sputter deposition system operated in a pulsed direct current (DC) mode. 1.5  $\mu\text{m}$  thick Al contact metallization pads are then formed on top of the AlN. The top Al electrodes are then formed. Finally, the Lamb wave devices are acoustically isolated from the supporting Si substrate by etching the Si substrate from the backside using a standard three-step dry etch Bosch process. The deposition of a 2.2  $\mu\text{m}$  thick AlN film having a 2.0 full with half maximum (FWHM) of the (002) X-ray rocking curve was made without external heating.

## II. ONE-PORT THIN FILM LAMB WAVE RESONATORS

In Fig. 3 the basic geometry of the micromachined thin film plate acoustic wave resonators (FPAR) is shown. It represents a one-port Lamb wave resonator employing IDT excitation.

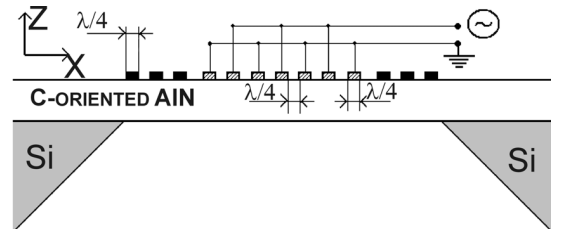


Figure 3. Lamb wave resonator topology.

The reflectors are formed by a quarter wavelength open-circuited Al strips periodically aligned on the top of the membrane surface. The reflectors are placed symmetrically at a wavelength distance from the IDT. The interdigital

transducer and the reflecting gratings have equal pitch  $\Lambda$  and metallization ratio  $m=a/\Lambda$ . A peculiarity of the synchronous FPARs utilizing the S0 mode in AlN plates is the fact that they operate in the vicinity of the upper stopband edge where the acoustic wave velocity in the grating exceeds the velocity in the outer area [1]. The latter is known to promote undesirable diffraction and to substantially decrease the device quality factor. One way to minimize the impact of the diffraction is to increase the device aperture. Three types of synchronous one-port lamb wave resonators having different apertures have been designed and micromachined in order to evaluate the influence of the aperture over the resonator response. The design parameters are summarized in table I. It is noted that all devices in this study are fabricated on one wafer and have an equal grating pitch and strip thickness  $h$ .

TABLE I. DESIGN PARAMETERS OF THE SYNCHRONOUS ONE-PORT LAMB WAVE RESONATORS

AlN: $d=2.2\mu\text{m}$ , Al electrodes thickness: $h=270\text{nm}$
$\lambda=12\mu\text{m}$ , $\Lambda=6\mu\text{m}$ , $m=0.42$ (targeted 0.5)
Strips in the Reflectors: $N_R=62$
Strips in the Transducers: $N_{IDT}=61$
Device Apertures: $W=30\lambda$ ; $40\lambda$ ; $50\lambda$ ;

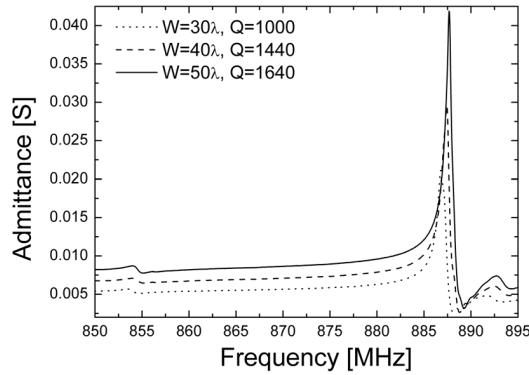


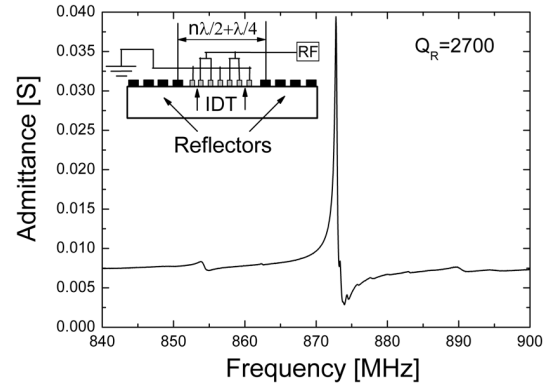
Figure 4. Close to resonance characteristics of IDT based FPARs having different apertures.

In Fig. 4 the close to resonance frequency response of the fabricated synchronous IDT based FPARs is shown. The existence of a stopband having a lower stopband edge situated at 853 MHz and an upper stopband edge at 888 MHz is clearly seen. All devices demonstrate a temperature coefficient of frequency TCF of around -20ppm. With the increase of the aperture the admittance expectedly increases in a linear fashion. The devices show an improvement in the measured

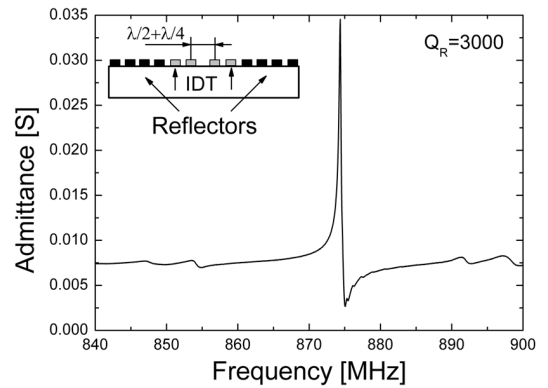
$$Q = \frac{f}{2} \left. \frac{\partial \varphi_z}{\partial f} \right|_{f_s} \quad (\varphi_z \text{ is the phase of the measured device}$$

impedance) with increasing aperture. Statistically the measurements on the entire wafer confirm this trend revealing a relatively big difference between the Q factors of devices having  $30\lambda$  and  $40\lambda$  apertures, respectively. On the average the  $50\lambda$  aperture devices demonstrate slightly higher Qs

compared to the  $40\lambda$  aperture devices. It is noted that the apertures cannot be arbitrary large because of the limited area of the thin film membranes that can practically be achieved. Accordingly, devices having apertures not significantly exceeding  $40\lambda$  are of practical interest. As it has been previously discussed [1], further improvements in the device Q can be achieved by designing them to operate inside the frequency stopband where the reflection coefficient reaches its maximum. The latter is usually achieved by slightly changing the distance between the two reflectors by a quarter wavelength. For the FPAR, however, this cannot be simply achieved because of the extremely strong reflections inside the transducer. Thus, the transducer itself represents a narrowband device operating in the vicinity of the upper stopband edge. In here, two approaches for achieving operation in the stopband center are presented. In the first approach the IDT with regular electrodes is replaced by a splitted electrode transducer having 3 electrodes per period and the distance between the reflectors is shifted by a quarter wavelength from the synchronous regime.



(a)



(b)

Figure 5. Close to resonance characteristics of IDT based FPARs operating in the vicinity of the stopband center. a) Splitted electrode geometry; b) Hiccup geometry

In Fig. 5a close to resonance frequency response of the fabricated asynchronous splitted IDT based FPAR having  $40\lambda$

aperture is shown. The IDT consists of 31 electrode pairs (93 electrodes) while the reflectors consist of 62 electrically shorted electrodes. The demonstrated  $Q=2700$  exceeds twice the  $Q$  characteristic for its synchronous counterpart (see Fig. 4). The second design approach for in-band operation utilizes a quarter wavelength shift introduced inside the regular electrode IDT, while the reflectors are placed synchronously around the IDT. More specifically the fabricated device has a  $50\lambda$  wide aperture, reflectors consisting of 62 electrodes and an IDT consisting of 62 electrodes with an internal gap of  $2.25\lambda$ . The measured device  $Q$  approaches 3000 at a frequency of about 875MHz (see Fig. 5b). This design is also beneficial because it enables the use of wider electrodes in the transducer and thus promotes lower parasitics in the structure. It is also noted that due to certain fabrication deficiencies the parasitic resistance in the structures is relatively high reaching values of around  $11\Omega$ . Avoiding this undesired effect seems to be trivial and most probably will result in devices with a much better performance.

### III. TWO-PORT THIN FILM LAMB WAVE RESONATORS

The basic topology of a two-port thin film plate wave resonator is shown in Fig. 6. Such resonators are IC compatible and can be used for example in low noise integrated feedback loop oscillators (FLO) or as integrated narrowband filters. In here an initial attempt to design and fabricate such types of devices is presented.

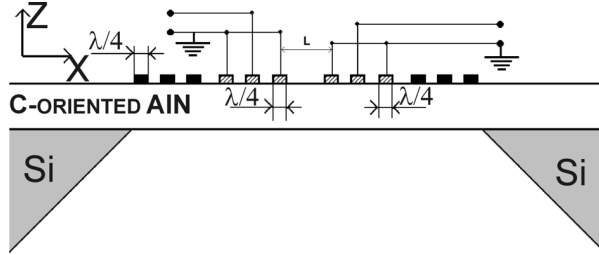
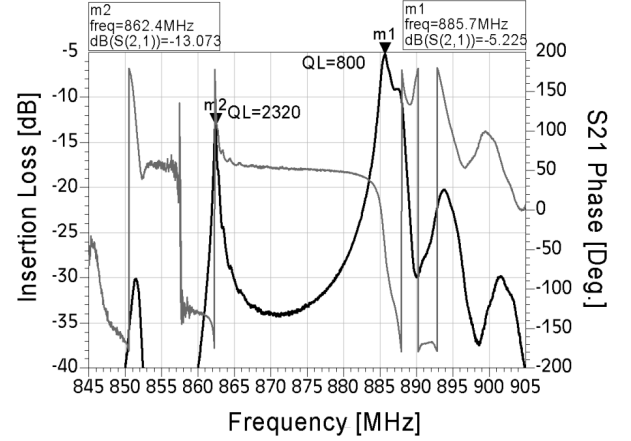


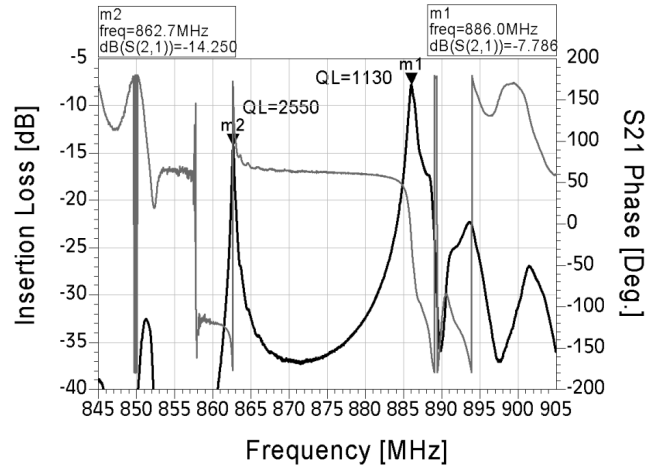
Figure 6. Two-port Lamb wave resonator topology.

The limited membrane dimensions challenge the design of two-port plate wave resonators. Thus the cavity length  $L$  can be increased at the expense of decreasing the number of strips in the reflectors and/or in the transducers. In Figure 7a,b the close to resonance characteristics of  $12\mu\text{m}$  wavelength ( $6\mu\text{m}$  pitch) two-port FPARs are shown. Both devices have a cavity length  $L=7.5\lambda$  and an aperture of  $50\lambda$ . The response shown in Fig. 7a corresponds to a device with 43 strips in the IDT ensuring good matching to  $50\Omega$  and 48 strips in the reflectors. The response shown in Fig. 7b corresponds to a device having longer reflector (64 strips) ensuring better reflectivity at the expense of the IDT dimensions (29 strips). The first device (see Fig. 7a) demonstrates an Insertion Loss of  $IL=5.2\text{dB}$ , Loaded  $Q_L=\pi f \tau$  (f- frequency,  $\tau$  - group delay) of 800 and corresponding unloaded  $Q_U=Q_L/[1-10^{-IL/20}]$  of 1770 at 885.7MHz resonance frequency. The peak observed in the vicinity of the lower stopband edge features  $IL=13.1\text{dB}$ ,  $Q_L=2320$  and corresponding  $Q_U=2982$  at a frequency of 862.4 MHz. The design with longer reflectors (see Fig. 7b) demonstrates an improved IL of 7.8dB due to the poorer

matching to  $50\Omega$ ,  $Q_L=1130$  and corresponding  $Q_U=1910$ . The peak observed in the vicinity of the lower stopband edge features  $IL=14.2\text{dB}$ ,  $Q_L=2550$  and corresponding  $Q_U=3160$  at a frequency of 862.7 MHz. Expectedly the improved reflectivity in the reflectors leads to higher values of the unloaded  $Q$  but poorer matching to the external load. This structure can be further optimized by designing it to operate in the vicinity of the stopband center as has been demonstrated above for the one-port FPARs.



(a)



(b)

Figure 7. Close to resonance S21 measurements on  $12\mu\text{m}$  wavelength two-port FPARs with: a) matched IDT b) Improved Reflectors

In Fig. 8 the measured close to resonance characteristics of a two-port Lamb wave resonator with a symmetrical topology are shown. In this topology one of the IDTs is splitted in two parts placed synchronously on either side of the second IDT. More specifically the device has an aperture of  $50\lambda$  and has 33 strips in the IDTs, 55strips in the reflectors while the distance between the IDTs is  $7\lambda$  on both sides. The area between the IDTs is electroded by a grating with the same pitch as that of the reflectors. The device demonstrate an  $IL=9.5\text{dB}$ ,  $Q_L=1100$  and a corresponding  $Q_U=1660$  at a resonance frequency of about 887.6 MHz. It is noted that the measured device characteristics are to some extent moderated

by the relatively high parasitic resistances achieved in this batch as discussed above. Again rectifying this deficiency is thought to result in a sufficient improvement in the performance. Further, design tools based on the coupling-of-modes theory can be employed for optimization of the design of two-port FPARs.

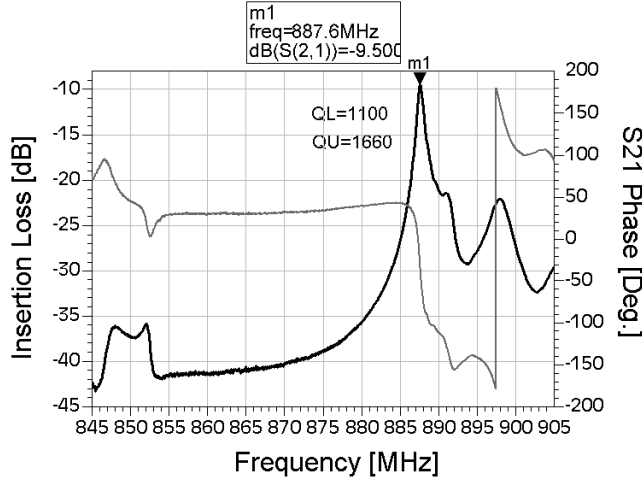


Figure 8. Close to resonance S21 measurements on 12 $\mu$ m wavelength two-port FPAR with symmetrically aligned IDTs

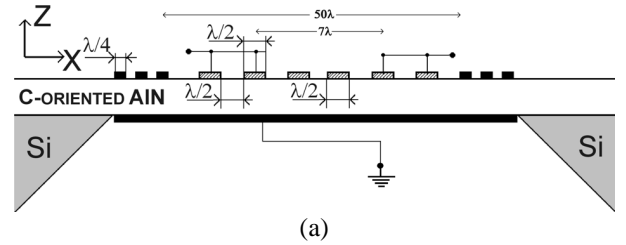
As previously discussed [1, 16] thin film Lamb wave resonators can benefit in electromechanical coupling if longitudinal wave transducers utilizing lateral field excitation (LW-LFE) are used instead of IDT. In Fig. 9a a schematic view of the fabricated 12 $\mu$ m wavelength two-port resonator utilizing LW-LFE transducers is shown. The device consists of 53 quarter wavelength electrodes with a 6 $\mu$ m pitch in the reflectors, 21 half-wavelength electrodes in the transducers (pitch 12 $\mu$ m) and 6 half-wavelength electrodes in the central grating. The distance between the reflectors is  $50\lambda$  while that between the transducers is  $7\lambda$ . In figure 9b the device as fabricated is shown. As seen from figure 9c the frequency response is more complex than anticipated. Two pronounced peaks in the vicinity of the resonance are seen. It is noted that the S21 phase differs substantially for both peaks. The major peak demonstrate an insertion loss as low as 2.44dB and  $Q_L=680$  corresponding to  $Q_U=2632$  at 854.8MHz. The parasitic resistance in this structure is less than  $2\Omega$ . The complex behavior is related to the difference between grating pitch of the reflectors on the one hand, and the transducers and the central grating on the other [1]. Deeper understanding of the propagation characteristics in such structures is needed for achieving more optimal designs. The synchronous design presented here does not seem to be the most optimal one.

#### CONCLUSIONS

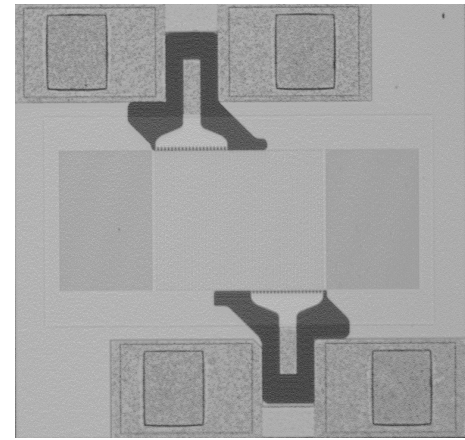
One-port resonators utilizing the lowest order symmetric lamb wave in thin AlN films operating in the vicinity of the stopband center are demonstrated in this work. Q factors as high as 3000 have been demonstrated for frequencies around 880MHz. Further, the devices are thought to exhibit an

improved performance provided the fabrication deficiencies resulting in increased parasitic resistances are eliminated.

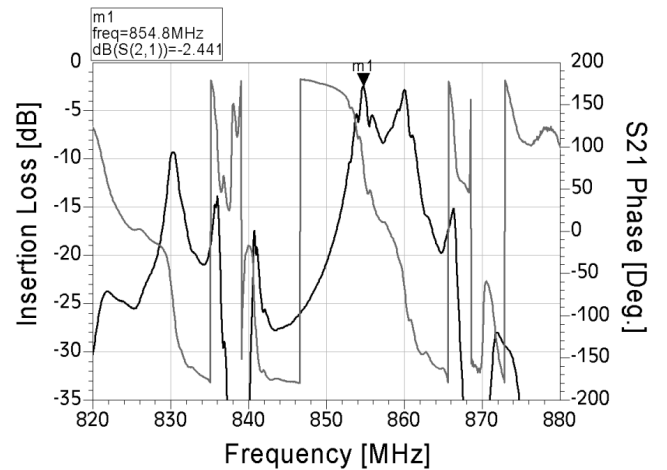
Thin film two-port resonators utilizing the S0 plate wave are demonstrated in here for the first time. An unloaded  $Q_U$  exceeding 3100 is demonstrated at frequencies around 850MHz. Initial results for two-port devices utilizing LW-LFE transducers are also shown. Unloaded  $Q_U$  exceeding 2600 is demonstrated at frequencies around 850MHz.



(a)



(b)



(c)

Figure 9 Two-port LW-LFE FPAR a) schematic; b) as fabricated; c) Close to resonance response

#### ACKNOWLEDGMENT

Prof. Viktor Plessky is highly acknowledged for his valuable comments.

# REFERENCES

- [1] V. Yantchev and I. Katardjiev, "Micromachined Thin Film Plate Acoustic Resonators Utilizing the Lowest Order Symmetric Lamb Wave Mode", IEEE Trans. UFFC., vol. 54, No.1, pp. 87-95, 2007
- [2] H. Matsumoto et. al., "Multilayer Film Piezoelectric Lamb Wave Resonator for several GHz Applications", Proc. 2006 Freq. Contr. Symp., pp. 797 – 800, 2006
- [3] Y. Nakagawa et. al., "Lamb wave type high frequency resonator", Jpn. J. Appl. Phys., vol. 42, pp. 3086-3090, 2003.
- [4] C. Campbell Surface Acoustic Wave Devices for Mobile & Wireless Commun.; Acad. Press. Inc., San Diego, USA, 1998.
- [5] K. Tsubouchi, N. Mikoshiba, "Zero-temperature-coefficient SAW devices on AlN epitaxial films", IEEE Trans. Son. Ultrason., SU-32, pp. 634-644, 1985.
- [6] K. Uehara, C. Yang, T. Shibata, S. Kim, S. Kameda, H. Nakase, K. Tsubouchi, "Fabrication of 5-GHz-Band SAW filter with atomically-flat-surface AlN on Sapphire" Proc. 2004 IEEE Ultrason. Symp., pp. 203-206, 2004.
- [7] H. Nakahata, A. Hachigo, K. Higaki, S. Fujii, S. Shikata, N. Fujimori, "Theoretical study on SAW characteristics of layered structures including a diamond layer", IEEE Trans. UFFC., vol. 42, pp. 362 – 375, 1995.
- [8] V. Mortet, O. Elmazria, M. Nesladek, J. Haen, G. Vanhoyland, M. Elhakiki, A. Tajani, E. Bustarret, E. Gheeraert, M. D'Olieslaeger, P. Alnot, "Study of aluminum nitride/freestanding diamond surface acoustic waves filters", Diam. Related Materials, vol. 12, pp. 723-727, 2003.
- [9] O. Elmazria, V. Mortet, M. Hakiki, M. Nesladek, P. Alnot, "High velocity SAW using aluminum nitride film on unpolished nucleation side of free-standing CVD diamond", IEEE Trans. on UFFC, vol. 50, No. 6, pp. 710 – 715, 2003.
- [10] M. Benetti, D. Cannata, F. Pietrantonio, V. Fedosov, E. Verona, "Theoretical and Experimental Investigation of PSAW and SAW properties of AlN films on isotropic diamond substrates" Proc. 2005 Ultrason. Symp., pp. 1868 – 1871, 2005.
- [11] G. Iriarte, F. Engelmark, V. Katardjiev, V. Plessky, V. Yantchev, "SAW COM-parameter extraction in AlN/Diamond Layered Structures" IEEE Trans. UFFC, vol. 50 (11), pp. 1542-1547, 2003.
- [12] J. Bjurström, I. Katardjiev, V. Yantchev, "Lateral-field-excited thin-film Lamb wave resonator", Appl. Phys. Lett. 86, 154103 1-3, 2005.
- [13] J. Bjurström, V. Yantchev, I. Katardjiev, "Thin film Lamb wave resonant structures – The first approach", Solid. State. Electron., 50, pp. 322-326, 2006.
- [14] V. Yantchev, J. Enlund, J. Bjurström, I. Katardjiev, "Design of high frequency piezoelectric resonators utilizing laterally propagating fast modes in thin aluminum nitride (AlN) films", Ultrasonics 45, pp. 208 – 212, 2006.
- [15] E. Adler, "Matrix methods applied to acoustic waves in multilayers", IEEE Trans. UFFC, vol. 37, pp. 485–490, 1990.
- [16] V. Yantchev, I. Katardjiev, "Quasistatic Transduction of the fundamental symmetric lamb mode in longitudinal wave transducers", Appl. Phys. Lett., 86, 154103 1-3, 2006
- [17] V. Yantchev, I. Katardjiev, "Propagation characteristics of the fundamental symmetric Lamb wave in thin aluminum nitride membranes with infinite gratings", J. Appl. Phys., 98, pp. 84910 1-7, 2005.